Heterogeneous Dynamics and Domains in Supercooled *o*-Terphenyl: A Single Molecule Study

Laura A. Deschenes and David A. Vanden Bout*

Department of Chemistry and Biochemistry and Texas Materials Institute, University of Texas, Austin, Texas 78712

Received: March 28, 2002; In Final Form: August 29, 2002

Single molecule spectroscopy was used to characterize the rotation of fluorescent probe molecules in supercooled *o*-terphenyl (OTP) just above the glass transition. Rotational motions of spatially isolated individual probe molecules were followed in real time, revealing dynamics that reflect a mosaic of spatially heterogeneous environments. The short-time molecular motions in each environment are found to be diffusional, taking place through a Brownian rotational process characterized by a single rotational correlation time τ_C. The distribution of rotational diffusion constants for the heterogeneous environments becomes larger as the temperature approaches T_g, manifesting increased heterogeneity as OTP is cooled toward the glass transition. After many molecular rotations, the molecule's rotational time changes abruptly. This switch appears instantaneous on the time scale of molecular rotation and is indicative of a rapid rearrangement of the molecule and its local environment. The time required for the environment to change, τ_{Ex}, is on average 15 times larger than the τ_C, and nearly 300 times slower than the α-relaxation time in OTP. The ensemble average correlation, $\langle\tau_C\rangle$, and exchange times, $\langle\tau_{Ex}\rangle$, show a similar temperature dependence, both of which are consistent with the temperature dependence predicted by the Debye Stokes Einstein equation.

Introduction

There is mounting evidence that spatial heterogeneities play a significant role in the anomalous dynamics observed in materials near the glass transition.[1] Experiment,[2−10] simulation,[11,12] and theory[13−17] demonstrate that spatial heterogeneity is crucial to a detailed understanding of glass-forming materials near T_g, and that spatially heterogeneous domains which encompass a distribution of dynamic properties are strongly implicated in the nonexponential dynamics characteristic of bulk relaxation measurements of materials near T_g. However, direct measurement of the properties of these heterogeneities has proven challenging.[18] This paper presents a detailed study of the properties, distribution, and temperature dependence of the spatially heterogeneous domains in the small molecule supercooled liquid *o*-terphenyl (OTP) measured by single molecule spectroscopy (SMS).[19] SMS provides unprecedented detail about the rates and mechanisms of molecular motion in spatially heterogeneous materials as it follows in real time the motions of a spatially isolated probe molecule rotating in the supercooled liquid matrix a few degrees above T_g.

OTP is the prototypical fragile glass-forming liquid, attractive for both its relatively simple structure and its stability as an equilibrated metastable supercooled liquid at room temperature. Like all fragile glass formers, its structural relaxation shows a sharp deviation from the normal exponential decay observed in normal liquids, which undergo simple Brownian rotational diffusion. The dynamics of OTP have been the subject of innumerable measurements using a wide variety of experimental techniques, including light scattering,[20,21] X-ray scattering,[22] neutron scattering[23−25] NMR,[2,26−28] ESR,[29] dielectric relaxation,[30,31] and probe relaxation methods,[7,32−35] with a particular emphasis on the dynamics that occur as the material is cooled toward the glass transition. The relatively weak intermolecular interactions in liquid OTP give it the character of a simple van der Waals liquid and have made it an attractive system for comparisons between experimental results and theoretical predictions of molecular and ensemble behavior near the glass transition.[20,25,36−38]

These previous studies provide a valuable background for the single molecule experiments described in this report. A variety of probe relaxation[32,33] and NMR[2,26] experiments have given evidence for dynamic spatial heterogeneities that play a significant role in the highly nonexponential relaxation dynamics measured in OTP near T_g. These dynamically selective measurements rely upon preselecting a subset of environments whose dynamics are slower or faster than the ensemble average relaxation, determining the lifetime of the heterogeneity from the amount of time required for this selected subset to reproduce bulk equilibrium dynamics. Single molecule spectroscopy extends this observation of subsets to its logical extreme, investigating the smallest functional subensemble: the environment occupied by a single molecule. SMS experiments follow molecular rotation in real time wherever a probe molecule is found, without preselecting a particular subset of dynamics, thus directly accessing the distribution of dynamics that occur in the different environments throughout the sample. By following the polarization-resolved emission of an isolated probe molecule for many rotations, a single molecule rotational correlation function can be constructed, giving a rotational correlation time that quantifies the time scale for molecular rotation. Measuring many molecules in different regions of the sample leads to a distribution of correlation times, thus probing the spatial heterogeneity responsible for nonexponential dynamics.

* Corresponding author. E-mail: davandenbout@mail.utexas.edu.

10.1021/jp025843m CCC: $22.00
Published on Web 10/15/2002

A determination of the distribution of the different dynamics that occur throughout the sample leads to a direct measurement of how the environments experienced by an individual molecule evolve as the glass transition approaches. Molecules that experience multiple environments during the course of the experiment provide a direct measurement of the lifetime of each heterogeneous environment. This environmental exchange time shows that the environmental heterogeneities are not static, as a single molecule may undergo several environmental exchanges through the course of its photochemical survival time. Further, dynamics observed between environmental switches lead to the unambiguous determination of the properties of an individual domain, without averaging over multiple molecules or environments.

Previous single molecule experiments in the glass-forming polymer poly(methyl acrylate)[5,6] have characterized important dynamics that occur on different time scales in spatially heterogeneous domains. On short times, molecular rotation occurs through a simple Brownian diffusion, which persists for many rotational correlation times. This normal diffusion is disrupted at long times by a drastic alteration in the local environment that causes a sudden change in the observed rotation rate as the molecular motions adapt to reflect the properties of the new environment. These abruptly changing environments cause the long-time rotational behavior of a single molecule to appear nonexponential even though its short-time behavior is diffusional at every time. Similar motions, time scales, and properties are seen in OTP, despite the vast structural and chemical differences between the two systems.

The rotational correlation times reported here are determined by the rotation of a large fluorescent probe dye (rhodamine 6G) dispersed in the OTP matrix. While the measured correlation times show the same temperature dependence as the structural (α-) relaxation,[39] the absolute times measured are more than an order of magnitude slower.[27] This result is consistent with previous studies of probe rotation in both OTP and polymeric glass-forming materials, where small probes are found to rotate on the same time scale as the α-relaxation, but large probes produce an inherently slower rotational correlation time.[34,40] Environmental exchange times are found to occur on time scales much longer than the measured rotational correlation times, where $\langle\tau_{Ex}\rangle \approx 15\langle\tau_C\rangle$. Thus, the environmental exchange time is found to be nearly 300 times longer than the α-relaxation, at temperatures ranging from T_g+2 K to T_g+10 K. This is in sharp contrast to solid-state NMR work by Sillescu et al. which found the exchange times at T_g+10 to be nearly identical to the OTP correlation time.[2] The current results are similar to what has been observed in polarization hole-burning experiments from Ediger et al. where exchange times 1000 times longer than the correlation time have been seen just above T_g.[33] However, in the hole-burning experiments, the exchange time is noted to shorten considerably as the temperature is increase.[32] The single molecule studies show very long exchange times at all temperatures. These discrepancies may be the result of using a large probe molecule or may indicate the single molecule experiments are probing a fundamentally different physical process.

Experimental Section

Single molecule experiments were performed using a home-built sample scanning inverted microscope described in detail in a previous publication.[5] The sample temperature was held constant in a liquid nitrogen cryostat (MicrostatN, Oxford Instruments). The temperature of the cryostat was measured using a thermocouple mounted to the sample holder. The small mass of the sample and cryostat allowed for rapid temperature stabilization and fluctuations of $<\pm 0.25$ °C. The operating pressure of less than 10 mTorr severely limited photochemistry due to reaction with oxygen. The cryostat was mounted atop a closed-loop x−y piezo scanning stage. The second harmonic of a Nd:YAG laser was used as an excitation source, focused to a diffraction-limited spot using a long working distance objective, while the fluorescence was collected through the same objective. A series of dichroic and long-pass filters were used to remove the excitation light before the fluorescence was split into two orthogonal polarizations using a polarizing cube beam splitter. The two resulting beams were imaged on the active area of two single photon counting avalanche photodiodes. Data collection and sample scanning were controlled using a home-built Labview (National Instruments) program.

OTP was purchased from Aldrich, distilled under vacuum, and passed through a membrane filter with 0.1 μm pores to remove any impurities capable of nucleating crystallization, resulting in a stable liquid that remains supercooled at room temperature for many months. Single molecule samples were prepared from OTP doped with small (0.1−1 nM) concentrations of the fluorescent laser dye rhodamine 6G. A small drop of the doped liquid was heated above the OTP melting point, pressed between two cover slides, and allowed to cool to room temperature, resulting in a 5−10 μm layer of dye-doped supercooled OTP between glass slides. The thickness and sample-to-sample variations of the OTP layer were measured in an optical microscope. Care was taken during sample preparation to ensure that the drop of OTP was small enough to avoid spreading to the edges of the cover slide in order to prevent crystallization at the sharp edge. Samples and stock solutions were stored in a vacuum desiccator when not in use, to prevent the uptake of atmospheric moisture.

Molecules are located spatially by imaging an area of the film; centering a molecule in the focus of the excitation beam, fluorescence transients can be recorded for as long as the molecule survives photochemically. The combined effect of low excitation powers and the removal of atmospheric oxygen from the system is extremely long-lived single molecules from which upward of 10^8 photons can be detected, thus permitting the dynamics of individual environments to be monitored for thousands of seconds. Transients were measured at temperatures 2, 5, and 10 K above the calorimetric glass transition for OTP (243 K) (determined by differential scanning calorimetry). For the lower temperatures, the very slow rotational dynamics permit long bin times of 1 s and extremely low excitation powers (0.02 μW) but still produce transients with good signal-to-noise. At T_g+10 K, when the average rotational dynamics occur on the time scale of a few seconds, bin times were necessarily reduced to 100 ms. As the majority of the background within 1 s dwells is dark noise from the detectors, the reduction of the dwell to 100 ms required only slightly higher excitation rates to produce transients with similar signal-to-noise. The increase in excitation intensity increased the photobleaching rate as well, reducing the average length of the measured transient from 5000 to 2200 s.

Measured transients consist of the fluorescence signals from the two orthogonal detectors. As the probes rotate freely in the OTP layer, the two signals vary smoothly with both anticorrelated fluctuations from probe rotation in the plane of the sample and correlated total intensity fluctuations as the molecule rotates out of the plane of the sample. The two fluctuating orthogonal signals $I_S(t)$ and $I_P(t)$, defined with respect to the beam-splitting

cube polarizations, are used to calculate the reduced linear dichroism $A(t)$:

$$A(t) = \frac{I_S(t) - I_P(t)}{I_S(t) + I_P(t)} = \cos(2\theta) \quad (1)$$

which is related to θ, the in-plane orientation of the probe molecule's transition dipole.[40] Because calculating $A(t)$ involves dividing by the total detected fluorescence intensity, it eliminates artifacts from laser fluctuation, triplet blinking,[41] spectral diffusion,[42] out-of-plane rotation, or translational diffusion away from the center of the excitation spot.

$A(t)$ is used to calculate the rotational autocorrelation function $C(t)$, with the standard method for discrete data points in finite time series:[43]

$$C(t) = \frac{\sum_{t'=0}^{T} A(t')A(t'+t)}{\sum_{t'=0}^{T} A(t')A(t')} \quad (2)$$

where T is the total number of points in the transient. $C(t)$ shows a monotonic decay which fits well to the Kohlrausch−Williams−Watts (KWW) "stretched exponential" function ubiquitous in the glass transition literature:

$$C(t) = \exp[-(t/\tau_{KWW})^{\beta}] \quad (3)$$

where $\beta = 1$ would reproduce a single exponential with time constant τ_{KWW}, but decreasing β indicates increasing heterogeneity with the addition of new, faster and slower time scale contributions. Rotation rates are conveniently described by the rotational correlation time τ_C, which combines τ_{KWW} and β into a single, weighted average time scale for rotation:

$$\tau_C = \int_0^{\infty} C(t)\, dt = \frac{\tau_{KWW}}{\beta}\Gamma\left(\frac{1}{\beta}\right) \quad (4)$$

Results and Discussion

Rotational Correlation Times. Figure 1 shows a typical single molecule transient for rhodamine 6G in OTP 5 K above the glass transition. Panel a depicts the two orthogonal polarization signals I_S and I_P, while panel b shows the calculated correlation function fit to the KWW equation, giving $\tau_{KWW} = 22.2 \pm 0.9$ s, $\beta = 0.847 \pm 0.04$, and $\tau_C = 24.2 \pm 1.8$ s. The chemical structures for OTP and rhodamine 6G are shown in panels c and d, respectively.

Because molecules rotate freely in three dimensions, they rotate out of the plane of the sample just as often as they rotate in the plane of the sample. These out-of-plane rotations appear in the transient as an intensity fluctuation, as out-of-plane rotation reduces the overlap between the exciting field and the molecular transition dipole. Isotropic rotational diffusion should produce out-of-plane signal fluctuations on the same time scales as the in-plane fluctuations. Although the two motions have the same average time scale, the motions themselves should not be correlated. To verify this fact, the autocorrelation function calculated from the reduced linear dichroism $A(t)$ was compared to the autocorrelation of the total fluorescence intensity $I_S(t) + I_P(t)$, and the cross-correlation between the two motions. For the purposes of taking correlation functions, the total fluorescence signal was adjusted to vary between −1 and 1 to scale

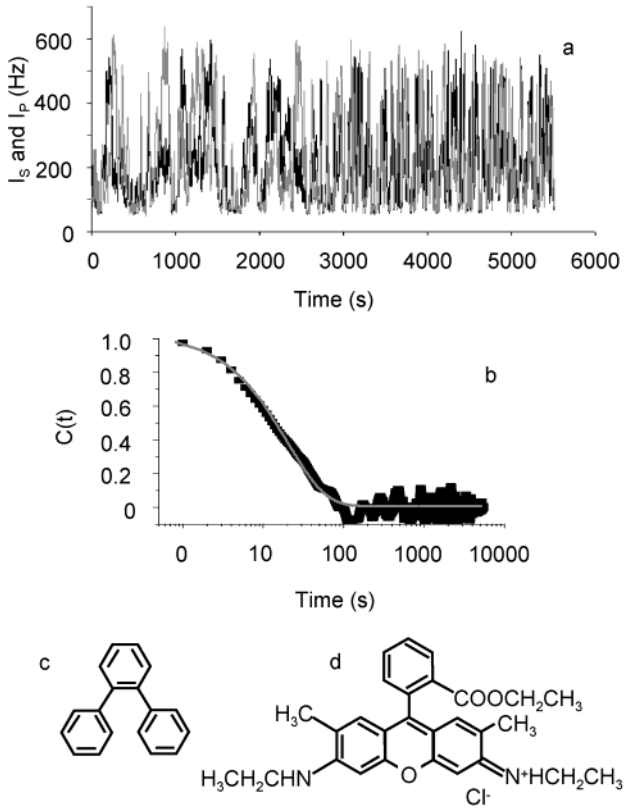

Figure 1. A rotational transient for rhodamine 6G in *o*-terphenyl at T_g+5 K. The two orthogonal fluorescence signals I_S and I_P (a) are used to calculate the rotational correlation function (b), fit with the KWW equation with $\tau_{KWW} = 22.2 \pm 0.9$ s, $\beta = 0.847 \pm 0.04$, and $\tau_C = 24.2 \pm 1.8$ s. The chemical structures of OTP and rhodamine 6G are shown in (c) and (d), respectively.

with $A(t)$. These correlation functions calculated for data at T_g+5 K are shown in Figure 2. The two signals $I_S(t)$ and $I_P(t)$ shown in (a) evince both in-plane and out-of-plane fluctuations. The normal autocorrelation of $A(t)$, shown in (b), is fit to the KWW function, resulting in $\tau_{KWW} = 24.6 \pm 1.0$ s, $\beta = 0.876 \pm 0.033$, $\tau_C = 26.26 \pm 1.2$ s, while the autocorrelation of the total intensity, shown in (c) and also fit to the KWW function, gives $\tau_{KWW} = 25.0 \pm 1.3$ s, $\beta = 0.883 \pm 0.042$, $\tau_C = 26.58 \pm 1.4$ s. These two decays reveal dynamics that are indistinguishable within the standard error in the fits. The cross-correlation between these two signals, shown in (d), is essentially zero. Thus, the in-plane and out-of-plane motions are independent and have the same correlation time, but the correlation time calculated from $A(t)$ and reflecting in-plane rotation is not correlated with the total intensity fluctuations. By measuring many molecules in the same sample, a distribution of single molecule correlation times can be compiled. By averaging over this distribution, the ensemble average correlation time $\langle\tau_C\rangle$ can be determined, where N is the total number of molecules studied.

$$\langle\tau_C\rangle = \frac{1}{N}\sum_{i=0}^{N-1}(\tau_C) \quad (5)$$

Temperature Dependence of the Rotation Times. The ensemble average correlation times determined by averaging individual molecules have been shown to reflect the bulk dynamics for polymer systems near the glass transition. [40] Figure 3a shows the ensemble average correlation time in OTP at three

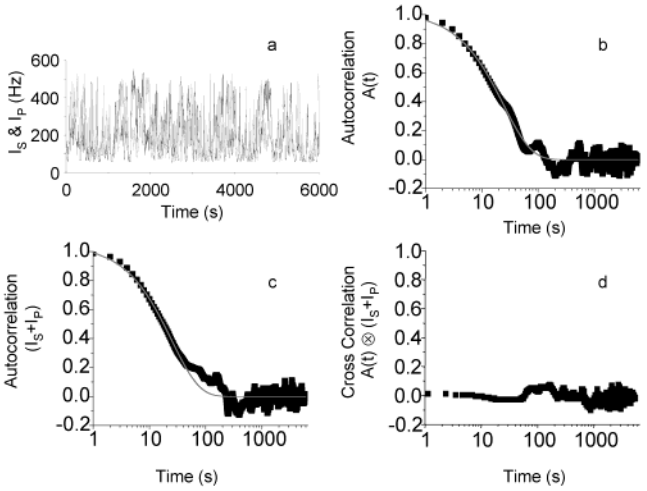

Figure 2. Isotropic rotation in three dimensions projected in the x−y plane. The polarized fluorescence signals $I_S(t)$ and $I_P(t)$ (a) show both anti-correlated intensity fluctuations from rotation in the $x-y$ plane and total intensity fluctuations from rotation out of the plane of the sample. These motions occur on the same time scale, but are independent of each other. The autocorrelation of in-plane motion is shown in (b), and fit to the KWW function, with $\tau_{KWW} = 24.6 \pm 1.0$ s, $\beta = 0.876 \pm 0.03$, $\tau_C = 26.2 \pm 1.2$ s. The autocorrelation for out-of-plane motion (c) is also fit to the KWW function, giving $\tau_{KWW} = 25.0 \pm 1.3$ s, $\beta = 0.88 \pm 0.042$, $\tau_C = 26.5 \pm 1.4$ s. The cross-correlation between the two motions (d) is essentially zero.

temperatures near T_g, where the solid line gives the Debye−Stokes−Einstein equation, which describes the temperature-dependent rotational motion of a solute in a solvent.

$$\tau_C = \frac{1}{D_{rot}} = \frac{4\pi\eta r_s^3}{3kT} \tag{6}$$

Here η is the viscosity of the solvent, r_s is the hydrodynamic radius of the rotating particle, and k is the Boltzmann constant. The hydrodynamic radius of rhodamine 6G is taken as 5.6 Å,[44] and the viscosity of OTP near the glass transition is well-known.[35] The error bars on the $<\tau_C>$ points show the standard deviation of the distribution of measured correlation times. This distribution reflects the spatial heterogeneity that leads molecules in different locations to have different dynamics. These environments are not static, however, as a molecule's environment can be seen to switch on a time scale many times longer than the rotational correlation time, but shorter than the photochemical lifetime of the molecule. These switches appear as abrupt changes in the rotation rate of the molecule. As the molecule is never observed to rotate on the time scale of this change, it is highly unlikely that the probe has simply moved into a new environment. This abrupt change in rotation rate must be the result of a collective rearrangement of the probe and its environment. These changes have a pronounced effect on the measured dynamics. As molecules may sample many different environments during the course of the experiment, the dynamics of the longest-lived molecules reflect an ensemble average over many different environments, and converge upon a bulklike ensemble average correlation time. Figure 3b−d plots the calculated correlation times against the photochemical survival time for the rhodamine molecule at 10, 5, and 2 K above T_g. At short times, the molecules show a broad distribution of correlation times as each samples only few environments throughout its lifetime, but as the molecules live longer they sample more environments, and converge upon a time average correlation time that is the same as the number averaged

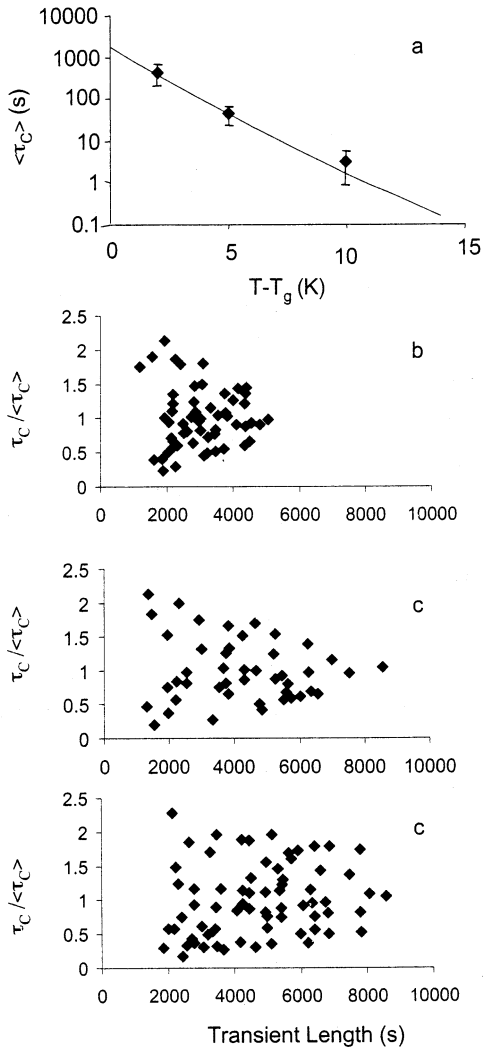

Figure 3. Ensemble average and single molecule rotational correlation times. Panel a shows ensemble average correlation times $\langle\tau_C\rangle$ as a function of reduced temperature, where the solid line gives Debye−Stokes−Einstein temperature scaling for solute rotation. Error bars give the standard deviation of the distribution of single molecule correlation times for transients of all lengths. Panels b through d show the distribution of single molecule correlation times τ_C normalized to the ensemble average correlation time $\langle\tau_C\rangle$ as a function of the photochemical survival time for the molecule at T_g+10 K, T_g+5 K, and T_g+2 K, respectively.

correlation time $<\tau_C>$. As the system more closely approaches the glass transition, each heterogeneous environment persists longer, as evinced by the growing time it takes the distribution to converge.

Environmental Exchange Times. The persistence time of these heterogeneous environments can be measured directly from single molecule data. While $A(t)$ is a convenient quantity for calculating correlation functions, a more intuitive measure of molecular rotation is the in-plane orientation θ of the transition dipole, which can be calculated from the orthogonal fluorescence signals by

$$\theta(t) = \arctan\left(\sqrt{\frac{I_S(t)}{I_P(t)}}\right) \tag{7}$$

Transitions between different environments appear as sharp changes in the rotation rate, and can easily be measured from the absolute value of the in-plane angle change. Although the

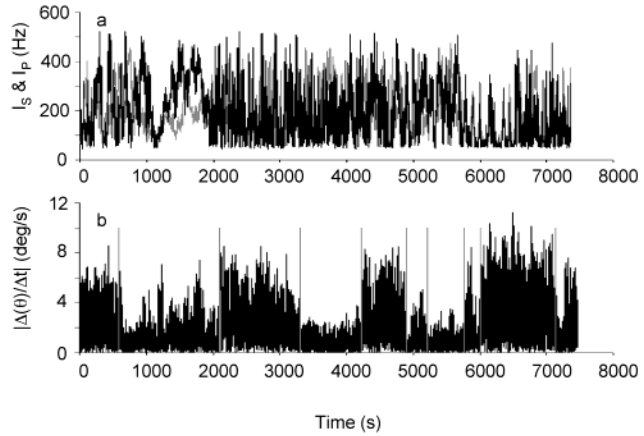

Figure 4. Determination of environmental exchange times for a long-lived single molecule in OTP at T_g+5 K. While the fluorescence intensity data (a) show some evidence of changing rotation rates, the exchanges are much clearer in the absolute value of the change in the in-plane orientation (b). Exchanges are demarcated with gray lines calculated using the criterion in eq 8.

precise point of exchange is difficult to resolve from the raw fluorescence signals, looking at the change in orientation with time makes the transitions between different rotation rates clearer. The durations of these segments of homogeneous rotation are determined by calculating a running average and standard deviation of the absolute change in angle with time over 10−20 time points, and comparing the standard deviation to the previous average. When the new average is more than 2 standard deviations different from the old average, the environment is considered to have changed.

$$\left|\frac{1}{N}\sum_{i=1}^{N}(x_i) - \frac{1}{N}\sum_{i=0}^{N-1}(x_i)\right| > 2\sqrt{\left(\frac{1}{N-1}\sum_{i=0}^{N}(x_i-\bar{x})^2\right)}$$

$$x = \frac{\Delta\theta}{\Delta t} \tag{8}$$

Figure 4 illustrates this determination; while the fluorescence intensities (a) show evidence of changing rotation rates, it is difficult to choose a definitive point at which the rate changes. However, exchanges appear as clear level changes in the absolute value of the angle change, and are demarcated in Figure 4b with gray lines determined using the criterion described in eq 8. The persistence time for a given environment, the environmental exchange time τ_{Ex}, can be measured directly from the time between switches. The distribution and temperature dependence of exchange times are shown in Figure 5, where panels a, b, and c show histograms of exchange times measured at T_g+10 K, T_g+5 K, and T_g+2 K, respectively. As the system is cooled toward the glass transition, the exchange time becomes longer, as shown in Figure 5d, which shows the ensemble average exchange time as a function of reduced temperature. The range indicated on these averages reflects the standard deviation of the distribution, demonstrating that in addition to becoming longer on average, the distribution of exchange times becomes broader as the glass transition is approached.

Temperature Dependence of the Exchange Times. The single molecule results show an ensemble average exchange time $\langle\tau_{Ex}\rangle$ much longer than $\langle\tau_C\rangle$, and with a temperature dependence slightly weaker than the correlation time. However at the lowest temperature measured, a significant population of exchange times approach the photochemical survival time for a rhodamine 6G molecule, suggesting that the measured

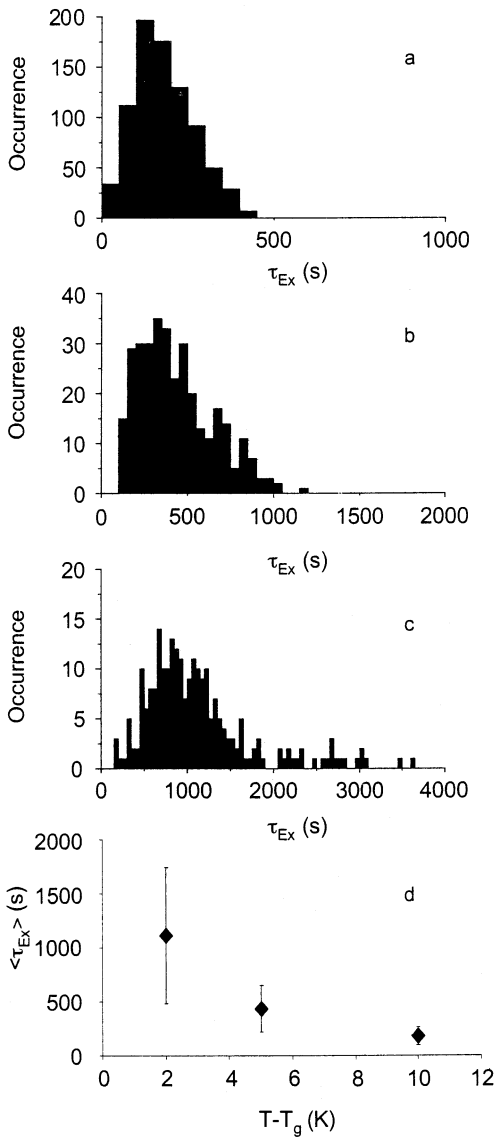

Figure 5. Distributions of environmental exchange times τ_{Ex} in OTP at T_g+10 K, T_g+5 K, and T_g+2 K (panels a through c, respectively), and the ensemble average exchange time $\langle\tau_{Ex}\rangle$ as a function of temperature, where the indicated range gives the standard deviation of the ensemble.

ensemble average at this temperature may be missing some of the longest exchanges and thus slightly skewed to shorter time. Indeed, nearly 8% of transients measured at this temperature show only one exchange event during their lifetime, preventing the measurement of the environmental lifetime. This being the case, it can be inferred that the environmental exchange times, reasonably corrected for the measurable ensemble, show a similar temperature dependence as the rotational correlation times. Without any correction, the exchange time normalized to the correlation time actually increases with increasing temperatures. That is not to say that it actually is longer at higher temperature, but relative to the correlation time it increases. It should be noted that at all the temperatures measured, the ensemble average exchange time, $\langle\tau_{Ex}\rangle$, is approximately 15 times longer than the ensemble average rotational correlation time, $\langle\tau_C\rangle$. The correlation time shows the same temperature dependence as the OTP α-relaxation, [39,45,46] but with an absolute time an order of magnitude slower. Thus, it is found that environmental exchange is between 200 and 300 times slower than the α-relaxation in OTP.

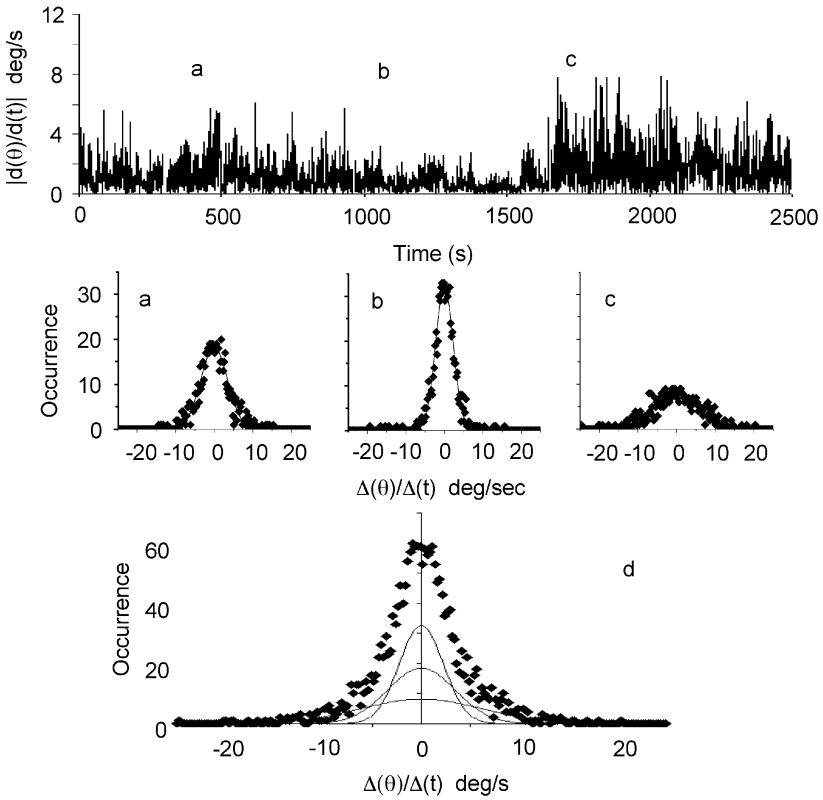

Figure 6. Diffusional dynamics between exchanges in OTP at T_g+5 K. A transient that makes several exchanges is shown at the top, with exchanges marked in gray according to eq 8. Panels a through c are histograms of the angle change per second for the regions between exchanges, marked a, b, and c. Each histogram is fit to a Gaussian distribution, yielding $\sigma = 6.9$, $\sigma = 4.5$, and $\sigma = 12.3$, respectively. Panel d gives the histogram of angle changes for the entire transient, fit with the amplitude-weighted sum of the Gaussian fits of the individual pieces. The gray line through the data represents this sum, while the black lines show the individual Gaussian components.

These results can be directly compared to previous measurements of environmental exchange in OTP. Polarization hole-burning experiments[7] by Ediger et al. have measured exchange times that are a thousand times longer than the correlation time near T_g.[33] However, this exchange becomes significantly shorter as the temperature is increased.[32] Solid-state NMR experiments by Sillescu et al. at T_g+10 K reveal exchange times that are comparable to the correlation time for OTP.[2] In contrast, the single molecule experiments observed environments that persist for 300 times longer than the α-relaxation time at T_g+10 K. There are several possible explanations for these differences. First, the single molecule experiments identify exchanges by discrete changes in rotation rate. There are potentially more subtle shifts in rotation rate that are not identified due to limited signal to noise in the experiments. This would bias the single molecule distribution of exchange times to longer times at all the temperatures. This would be most pronounced at the highest temperatures where the dynamics are the fastest. However, it is unlikely that this would account for all of the large difference between the SMS and NMR results. A second possibility is that the large probe molecule used in the single molecule experiment is affecting the dynamics of the environments. In both the hole-burning and NMR experiments, the ensemble relaxation was characterized by a KWW decay with a β value near 0.6. For the single molecule experiments, the average rotational correlation function for rhodamine 6G gives a KWW decay with a β value near 0.8. The larger β value is a clear indication that the probe is not sampling the full distribution of the heterogeneity available in the neat OTP. The large size of the probe molecule may be washing out environmental exchanges that occur on smaller distance scales and on faster time scales. This question is currently being addressed by single molecule experiments in OTP with small probe molecules.

Correlation Times for Single Environments. The single molecule measurement of the exchange time τ_{Ex} provides a direct measurement of how long a molecule stays in a particular heterogeneous microenvironment. The details of the dynamics within a single environment can be found from analysis of transient segments identified between environmental exchanges. The rotational correlation function, while useful for describing the time-averaged rotational dynamics for a single molecule, gives an accurate picture of the short time dynamics only in the rare situation that a single environment persists for enough rotations to provide good statistics on a calculated autocorrelation. In an early study of single molecule rotations near T_g, a fortuitous combination of fast dynamics and a long exchange time gave a correlation function for a short subset of a transient that showed the single-exponential decay indicative of Brownian rotational diffusion,[6] but short exchanges and slow rotations thwart attempts to characterize most single environments using correlation functions. A more fruitful approach to this problem involves the direct measurement of the change in the in-plane orientation angle per unit time. For a rotational process governed by Brownian rotational diffusion, a histogram of angle changes should produce a Gaussian distribution of angle changes.

$$y = A \exp\left[\frac{-(x - x_c)^2}{2\sigma^2}\right] \tag{9}$$

where x_c, the center position of the Gaussian and the most probable (average) angle change per second, is 0, and σ gives the standard deviation of the distribution. While the mathemati-

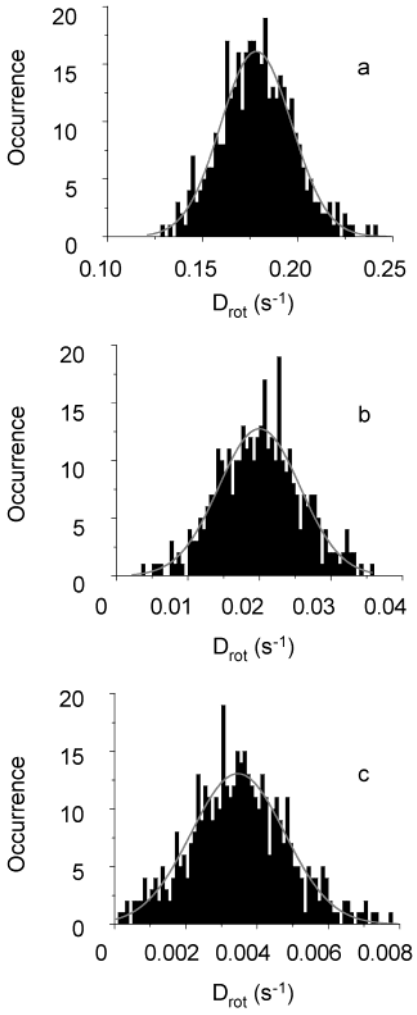

Figure 7. Distributions of rotational diffusion times for rhodamine 6G in OTP. Data in panels a through c are measured at T_g+10 K, T_g+5 K, and T_g+2 K, respectively

cal construct of a random walk involves infinitesimally small time steps with unit displacements in either the positive or the negative direction, any experimental sampling of a Brownian process will average over many infinitesimal time steps at each measurement time point. The averaging together a great many unitary displacements produces a Gaussian distribution of displacements centered at zero.

For transients analyzed between exchanges, it is found that all the histograms of the angle changes fit well to a Gaussian, indicating that all short-time dynamics are diffusional. Representative data in OTP at T_g+5 K are shown in Figure 6, where the top panel shows the absolute value of the angle change for a transient that makes several clear exchanges, as described by eq 8, and marked in gray. The change in angle per second for each of these environments, labeled a, b, and c, is plotted in a corresponding histogram. Each fits well to a Gaussian distribution, with $\sigma = 6.9$, $\sigma = 4.5$, and $\sigma = 12.3$, respectively. A histogram of the entire transient, shown at the bottom, is well represented by the amplitude-weighted sum of the three individual Gaussian fits. The individual curves are plotted for comparison, along with their sum, which runs through the points.

Because the dynamics within each environment are found to be diffusional, analysis of the distributions of displacements can provide insight into the properties of each environment. For a diffusional process, the mean-squared displacement can be related directly to the diffusion constant; for rotational diffusion, the relevant displacement is the change in orientation θ over a time period t.

$$\left\langle \frac{\theta^2}{t} \right\rangle = 2D_{rot} \tag{10}$$

From mean-squared angle changes measured between exchanges, the distribution of rotational diffusion constants for individual environments can be directly calculated. This distribution of diffusion constants is shown in Figure 7, where each is fit to a Gaussian. This likely is the result of the large probe molecule. The KWW distribution for a β value near 0.8 is not strongly asymmetric. Although the width of the distribution and the average diffusion constant change with temperature, the shape of the distribution is invariant with temperature. The average diffusion constant determined by the Gaussian fit varies from 0.178 to 0.020 to 0.0035 s^{-1} as the temperature is cooled from T_g+10 to T_g+5 to T_g+2 K, while the standard deviation goes from 0.019, to 0.0057, to 0.0013. This represents the expected behavior that occurs as the temperature is cooled toward T_g: the average dynamics become slower, but the distribution of accessible environments becomes larger. As a test of self-consistency, the distribution of rotational diffusion constants was converted into a distribution of rotational correlation times. The ensemble average correlation time calculated from the distribution of diffusion constants for individual environments reproduces the ensemble average correlation time measured from fitting rotational autocorrelation functions for single molecules.

Conclusions

Single molecule measurements of rotational dynamics in OTP at temperatures near the glass transition show the distinctive hallmark of spatially heterogeneous dynamics: molecules have different rotation rates in different locations. Short-time diffusional rotations are punctuated by distinct environmental changes that result in a new diffusional rotation rate. The distribution of single molecule correlation times depends strongly on the photochemical survival time of the fluorescent probe molecule; this dependence is the direct result of environmental exchanges in which the molecule and its environment rearrange. Ensemble average times for both environmental exchange and rotational correlation give a temperature dependence described by the Debye−Stokes−Einstein equation. However, environmental exchange occurs much more slowly than does probe rotation, with $\langle\tau_{Ex}\rangle \approx 15\langle\tau_C\rangle$. Since correlation times measured using the large probe dye rhodamine 6G are more than an order of magnitude longer than the OTP α-relaxation, environmental exchanges are found to be roughly 300 times slower than the α-relaxation time at temperatures ranging from T_g+2 K to T_g+10 K. The results are different from what has been previously observed for exchange times in dynamically selective experiments. The results are similar to other probe studies just above Tg, but differ significantly from NMR work at higher temperatures. This is likely due to the large size of the probe molecule and suggest the need for further single molecule work with different probes.

Because environmental exchanges are clearly apparent as changes in the molecular rotation rate, the dynamics that occur between exchanges give a direct measurement of the properties of individual heterogeneous environments. Rotational dynamics in individual environments are found to fit well to Gaussian distributions of incremental angle changes, confirmation that molecular rotation in a single environment occurs through

a normal diffusional Brownian rotational motion. In addition, the distribution of diffusion constants grows broader with decreasing temperature, indicating that OTP becomes more heterogeneous as it approaches the glass transition. The time scales and kinds of molecular motion observed in OTP bear a striking resemblance to results from single molecule experiments in polymeric glass-forming materials, though the liquid and polymer materials have very different physical and molecular properties.

The single molecule work taken along with previous study of heterogeneous dynamics yields the emerging picture of the dynamics of OTP just above the glass transition; the liquid is composed of a mosaic of heterogeneous regions, each of which behaves just like a normal liquid with a single well-defined rotational diffusion constant. While previous studies had demonstrated clear evidence of heterogeneity, the single molecule experiments provide greater insight into the details of that heterogeneity. Specifically, by probing individual environments, it is clear that within a given environment the dynamics are purely diffusional. This is observed both in the exponential decays of rotational correlation functions at short times and in the Gaussian distribution of angle changes observed for discrete environments. Last the single molecule experiments show that the molecules reside in one of these environments for many correlation times but then change abruptly to show diffusional motion on a new time scale. In conclusion, the single molecule probe studies can provide new details of molecular motion in liquids near the glass transition. However, much work remains in understanding the role of the probe in the measurements and how to directly compare the time scales measured in the single molecule studies with other experimental methods.

Acknowledgment. D.A.V.B. gratefully acknowledges the Camille and Henry Dreyfus Foundation for a New Faculty Award. This work was supported by grants from the Research Corporation. D.A.V.B. is a Research Corporation Cottrell Scholar.

References and Notes

(1) Sillescu, H. *J. Non-Cryst. Solids* **1999**, *243*, 81−108.
(2) Böhmer, R.; Hinze, G.; Diezemann, G.; et al. *Europhys. Lett.* **1996**, *36*, 55−60.
(3) Böhmer, R.; Chamberlin, R. V.; Diezemann, G.; et al. **1998**.
(4) Reinsberg, S. A.; Qui, X. H.; Wilhelm, M.; et al. *J. Chem. Phys.* **2001**, *114*, 7299−7302.
(5) Deschenes, L. A.; VandenBout, D. A. *J. Phys. Chem. B* **2001**, *105*, 11978−11985.
(6) Deschenes, L. A.; VandenBout, D. A. *Science* **2001**, *292*, 255−258.
(7) Ediger, M. D. *Annu. Rev. Phys. Chem.* **2000**, *51*, 99−128.
(8) Weeks, E. R.; Crocker, J. C.; Levitt, A. C.; et al. *Science* **2000**, *287*, 627−630.
(9) Richert, R. *J. Phys. Chem. B* **1997**, *101*, 6323−6326.
(10) Tracht, U.; Wilhelm, M.; Heuer, A.; et al. *Phys. Rev. Lett.* **1998**, *81*, 2727−2730.
(11) Donati, C.; Douglas, J. F.; Kob, W.; et al. *Phys. Rev. Lett.* **1998**, *80*, 2338−2341.
(12) Bennemann, C.; Donati, C.; Baschnagel, J.; et al. *Nature* **1999**, *399*, 246−249.
(13) Adam, G.; Gibbs, J. H. *J. Chem. Phys* **1965**, *43*, 139−146.
(14) Chamberlin, R. V.; W., K. D. *J. Non-Cryst. Solids* **1994**, *172*−*174*, 318−326.
(15) Kivelson, S. A.; Zhao, X.; Kivelson, D.; et al. *J. Chem. Phys.* **1994**, *101*, 2391−2397.
(16) Xia, X.; Wolynes, P. G. *J. Phys. Chem. B* **2001**, *105*, 6570−6573.
(17) Xia, X.; Wolynes, P. G. *Phys. Rev. Lett.* **2001**, *86*, 5526−5529.
(18) Angell, C. A.; Ngai, K. L.; McKenna, G. B.; et al. *J. Appl. Phys.* **2000**, *88*, 3113−3157.
(19) Kelley, A. M.; Michalet, X.; Weiss, S. *Science* **2001**, *292*, 1671.
(20) Steffen, W.; Patkowski, A.; Gläser, H.; et al. *Phys. Rev. E* **1994**, *49*, 2992−3002.
(21) Patkowski, A.; Fischer, E. W.; Steffen, W.; et al. *Phys. Rev. E* **2001**, *63*, 061503.
(22) Patkowski, A.; Thurn-Albrecht, T.; Babachowicz, E.; et al. *Phys. Rev. E* **2000**, *61*, 6909−6913.
(23) Tölle, A.; Wuttke, J.; Schrober, H.; et al. *Eur. Phys. J. B* **1998**, *5*, 231−236.
(24) Bartsch, E.; Fujara, F.; Legrand, J. F.; et al. *Phys. Rev. E* **1995**, *52*, 738−745.
(25) Bartsch, E.; Bertagnolli, H.; Chieys, P.; et al. *Chem. Phys.* **1993**, *169*, 373−378.
(26) Böhmer, R.; Chambelin, R. V.; Diezemann, G.; et al. *J. Non-Cryst. Solids* **1998**, *235*−*237*, 1−9.
(27) Chang, I.; Fujara, F.; Geil, B.; et al. *J. Non-Cryst. Solids* **1994**, *172*−*174*, 248−255.
(28) Heuer, A.; Wilhelm, M.; Zimmermann, H.; et al. *Phys. Rev. Lett.* **1995**, *75*, 2851−2854.
(29) Andreozzi, L.; Cianflone, F.; Donati, C.; et al. *J. Phys.: Condens. Matter* **1996**, *8*, 3795−3809.
(30) Dixon, P. K.; Wu, L.; Nagel, S. R.; et al. *Phys. Rev. Lett.* **1990**, *65*, 1108−1111.
(31) Wu, L.; Nagel, S. R. *Phys. Rev. B* **1992**, *46*, 11198−11200.
(32) Wang, C.-Y.; Ediger, M. D. *J. Phys. Chem. B* **1999**, *103*, 4177−4184.
(33) Cicerone, M. T.; Ediger, M. D. *J. Chem. Phys.* **1995**, *103*, 5684−5692.
(34) Cicerone, M. T.; Blackburn, F. R.; Ediger, M. D. *J. Chem. Phys.* **1995**, *102*, 471−479.
(35) Cicerone, M. T.; Ediger, M. D. *J. Phys. Chem.* **1993**, *97*, 10489−10497.
(36) Mossa, S.; Ruocco, G.; Sampoli, M. *Phys. Rev. E* **2001**, *64*, 021511.
(37) Tölle, A.; Schober, H.; Wuttke, J.; et al. *Phys. Rev. E* **1997**, *56*, 809−815.
(38) Bendler, J. T.; Shlesinger, M. F. *J. Phys. Chem.* **1992**, *96*, 3970−3973.
(39) Hodge, I. M.; O'Reilly, J. M. *J. Phys. Chem. B* **1999**, *103*, 4171−4176.
(40) Deschenes, L. A.; Bout, D. A. V. *J. Chem. Phys.* **2002**, *116*, 5850−5856.
(41) Veerman, J. A.; Garcia-Parajo, M. F.; Kuipers, L.; et al. *Phys. Rev. Lett.* **1999**, *83*, 2155−2158.
(42) Lu, H. P.; Xie, X. S. *J. Phys. Chem. B* **1997**, *101*, 2753−2757.
(43) Box, G. E. P.; Jenkins, G. M. *Time Series Analysis Forecasting and Control*; Holden-Day: San Francisco, 1976.
(44) Porter, G.; Sadkowski, P. J.; Tredwell, C. J. *Chem. Phys. Lett.* **1977**, *49*, 416−420.
(45) Hwang, Y.-H.; Shen, G. Q. *J. Phys.: Condens. Matter* **1999**, *11*, 1435−1462.
(46) Plakek, D. J.; Bero, C. A.; Chay, I.-C. *J. Non-Cryst. Solids* **1994**, *172*−*174*, 181−190.